

Calculation of the Linear-Absorption Spectrum of an Ideal Two-Dimensional System of MoS_2

Presenter

Vo Chau Duc Phuong ¹

Supervisors

Dr. Huynh Thanh Duc ²

¹University of Science, Ho Chi Minh city

²Institute of Applied Mechanics and Informatics

December 9, 2024

Table of Contents

- 1 Transition Metal Dichalcogenide Structure and Properties
- 2 Exciton
- 3 Tight-binding Model
- 4 Semiconductor Bloch Equations
- 5 Numerical Results
- 6 Summary and Outlook

Transition Metal Dichalcogenide Monolayer

Transition metal dichalcogenide (TMD) is the compound has the form of MX_2 .

			Ti	V											S		
			Zr	Nb	Mo					Pd					Se		
			Hf	Ta	W	Re				Pt					Te		
Transition Metal										Chalcogenides							

Figure: Transition metal dichalcogenide compound, M is a transition metal atom and X is a chalcogenides atoms

Transition Metal Dichalcogenide Monolayer

Some of the combination don't have the stable monolayer form. Others can be:

- H (Honeycomb) structure (Example: MoS_2)
- T (centered honeycomb) structure (Example: NbS_2)

or both (Example: VS_2).

These structure can affect the properties of the materials. TMD can be either metal (NbS_2 , NbSe_2 -T) or semiconductor (MoS_2)¹.

My thesis focused on MoS_2 monolayer (only have the H-structure), has the visible band gap in the band structure, which can be used in creating the transistor devices.²

¹Ataca, Şahin, and Ciraci, "Stable, Single-Layer MX₂ Transition-Metal Oxides and Dichalcogenides in a Honeycomb-Like Structure".

²Radisavljevic et al., "Single-layer MoS_2 transistors".

Mono-layer structure

- The M (huge black dot) layer has been sandwiched by two X (small green dot) layers as shown in top view (a) and side view (b).
- They have the inverse asymmetry in real lattice.
- The atomic lattice have the D_{3h} symmetry group, result in the hexagon Brillouin Zone (BZ).

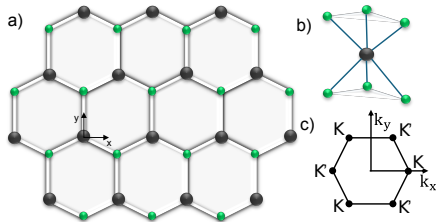


Figure: Structure and Brillouin Zone of Monolayer TMD, redrawing from³

³Liu et al., “Three-band tight-binding model for monolayers of group-VIB transition metal dichalcogenides”.

Splitting In The Band Structure

Huge split Δ (hundreds of meV) in valley (K and -K points) of the band structure caused by the strong spin-orbit coupling (SOC) and the inversion asymmetry.

⇒ Applications in spintronic and optoelectronics⁴.

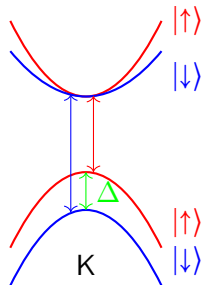


Figure: The allowed optical transition

⁴Liu et al., "Electronic structures and theoretical modelling of two-dimensional group-VIB transition metal dichalcogenides".

Creation of An Exciton

When an electron transit from valence band to a conduction band, it leave behind a hole.

This hole, acts like an positive charge, attract electrons to form a binding (called exciton).

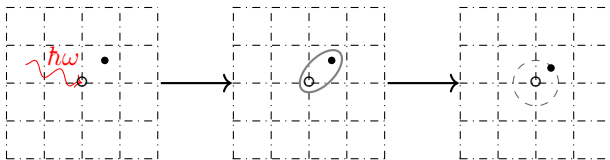


Figure: Illustration for the bouncing of the electron (black) and hole (circle)

Binding Energy of Exciton

Interaction between a couple of electron and hole can be described as "a Hydrogen" atom, called "Exciton".

$$-\left[\frac{\hbar^2 \nabla_{\mathbf{r}}^2}{2m_r} + V(r)\right]\psi_{\nu}(\mathbf{r}) = E_{\nu}(\mathbf{r})\psi_{\nu}(\mathbf{r}), \quad (1)$$

where,

- $V(r)$ is the Coulomb interaction with the form:

$$V(r) = \frac{e^2}{\varepsilon|\mathbf{r}|} \quad (2)$$

- $m_r = \frac{m_h m_e}{m_h + m_e}$ is the effective mass.
- $E_{\nu}(\mathbf{r})$ is the binding energy of the exciton.

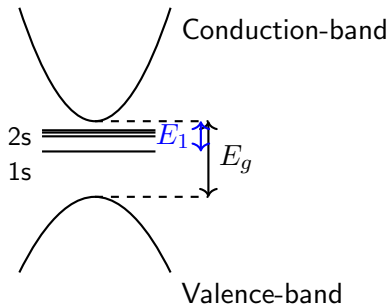


Figure: Binding energy relative to the band gap

Exciton

The Coulomb interaction in the form of Eq. (2) can only be valid if the bohr radius of "the Hydrogen-atom" around or smaller than the unit cell.

In the bulk crystals with relative small dielectric constant, the exciton have the small binding energy.

Ex: GeAs⁵:

$$E_b \approx 4.8 meV \ll E_g = 1.2 - 1.7 eV$$

In these materials, the exciton binding energy can be neglected in simulations.

⁵Diakite et al., *Accurate Electronic, Transport, and Bulk Properties of Gallium Arsenide (GaAs)*.

Purpose

So, why need to calculate it in TMD?

- In the 2-D materials (monolayer-TMD materials are in this), lack of system dimension causes decrease in the dielectric screening.
- Large quantum confinement in nano-material (z-axis).

⇒ Increasing of exciton binding energy. Larger magnitude about two orders in compared with bulk semiconductor.

- Previous theories predict binding energy too large ($0.5 - 1 \text{ eV}$), precisely experiment predicts significant smaller binding energy ($0.2 - 0.5 \text{ eV}$).
- Find a model not only simple but also precise enough for further research and application in industrial.

⇒ Look like enough for my bachelor's thesis 😊.

Tight-binding Model

Start from the Hamiltonian for an independence electron:

$$H_{1e}(\mathbf{r}) = -\frac{\hbar^2 \nabla^2}{2m} + \sum_{\mathbf{i}} V(\mathbf{r} - \mathbf{R}_i - \mathbf{r}_c), \quad (3)$$

where \mathbf{R}_i is the Bravais lattice position, \mathbf{r}_c is the relative position of atom inside unit cell. We neglected the motion of nucleus because in this case, the nucleus (Transition metals and Chalcogenides) are very heavy in compare with the electron (Born-Oppenheimer approximation).

Assuming that the electron stay close to its atom and have little overlap on the neighboring sites. Therefore the wave function of each electron can be described by the linearly combination of atomic orbitals (LCAO).

$$\psi(\mathbf{r}) = \sum_{n=1}^N \sum_{c=1}^{N_c} \sum_{\alpha=1}^{N_{orbital}} c_{\alpha c}(\mathbf{R}_n) \phi_{\alpha}(\mathbf{r} - \mathbf{R}_n - \mathbf{r}_c) \quad (4)$$

N , N_c , and N_{α} is number of unit lattice of the system, number of atom in a basis and number of orbital of an atom, respectively.

From LCAO wavefunctions, Bloch wavefunction can be constructed as:

$$\psi_{\mathbf{k}}(\mathbf{r}) = \sum_{c=1}^{N_c} \sum_{\alpha=1}^{N_{orb}} c_{\alpha c}(\mathbf{k}) e^{i\mathbf{k}(\mathbf{R}_n + \mathbf{r}_c)} \sum_{n=1}^N \phi_{\alpha}(\mathbf{r} - \mathbf{R}_n - \mathbf{r}_c). \quad (5)$$

Substituting (5) into Schrödinger equation with Hamiltonian (3), multiply with $e^{-i\mathbf{k}\mathbf{r}_c} \phi_{\alpha'}^*(\mathbf{r} - \mathbf{r}_{c'})$ and taking the integral on \mathbf{r} :

$$\sum_{c=1}^{N_c} \sum_{\alpha=1}^{N_{orb}} (H_{\alpha'c',\alpha c}(\mathbf{k}) - \varepsilon(\mathbf{k}) S_{\alpha c, \alpha'c'}(\mathbf{k})) C_{\alpha c}(\mathbf{k}) = 0, \quad (6)$$

In which

$$H_{\alpha'c',\alpha c} = \sum_{n=1}^N e^{i\mathbf{k}(\mathbf{r} + \mathbf{r}_c - \mathbf{r}_{c'})} \langle \phi_{\alpha}(\mathbf{r} - \mathbf{r}_{c'}) | H_{1e} | \phi_{\alpha'}(\mathbf{r} - \mathbf{R}_n - \mathbf{r}_c) \rangle \quad (7)$$

$$S_{\alpha'c',\alpha c} = \sum_{n=1}^N e^{i\mathbf{k}(\mathbf{r} + \mathbf{r}_c - \mathbf{r}_{c'})} \langle \phi_{\alpha}(\mathbf{r} - \mathbf{r}_{c'}) | \phi_{\alpha'}(\mathbf{r} - \mathbf{R}_n - \mathbf{r}_c) \rangle \quad (8)$$

If we approximate the overlapping matrix elements $S_{\alpha c, \alpha' c'}(\mathbf{k}) \approx \delta_{\alpha \alpha'} \delta_{cc'}$ (no overlapping between two difference atoms), we have (6) in the form of:

$$\sum_{c=1}^{N_c} \sum_{\alpha=1}^{N_{orb}} H_{\alpha' c', \alpha c}(\mathbf{k}) C_{\alpha c}(\mathbf{k}) = \varepsilon(\mathbf{k}) C_{\alpha c}(\mathbf{k}) \quad (9)$$

In semi-empirical formalism, Hamiltonian matrix elements are defined by the phenomenological "On-site energy" and "Hopping energy" parameters.

So, if we have the Hamiltonian matrix, we can solve it for eigenvalues and corresponding eigenvectors.

But, how to use it?

Second Quantization Hamiltonian

The second quantization Hamiltonian in basis of Bloch function $\{|\psi_{\lambda\mathbf{k}}\rangle\}$ for many electrons system with Coulomb interaction in the electromagnetic field in velocity gauge ($\phi = 0$)

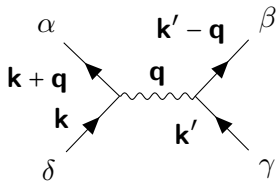
$$\begin{aligned} H &= H_{1e}^0 + H^{Coul.} + H^{e-L} \\ &= \sum_{\lambda\mathbf{k}} \varepsilon_{\lambda}(\mathbf{k}) c_{\mathbf{k}}^{\dagger} c_{\mathbf{k}} + \frac{1}{2} \sum_{\mathbf{k}\mathbf{k}'\mathbf{q}} \sum_{\alpha\beta\gamma\delta} V_{\mathbf{k},\mathbf{k}',\mathbf{q}}^{\alpha\beta\gamma\delta} c_{\alpha\mathbf{k}+\mathbf{q}}^{\dagger} c_{\beta\mathbf{k}'-\mathbf{q}}^{\dagger} c_{\gamma\mathbf{k}} c_{\delta\mathbf{k}'} \\ &\quad + \sum_{\lambda\lambda'\mathbf{k}\mathbf{k}'} \langle \psi_{\lambda\mathbf{k}} | \frac{e}{m} \mathbf{A}(\mathbf{r}, t) \cdot \mathbf{p} | \psi_{\lambda'\mathbf{k}'} \rangle c_{\lambda\mathbf{k}}^{\dagger} c_{\lambda'\mathbf{k}'} + O(\mathbf{A}^2) \end{aligned} \quad (10)$$

in which the creation $c_{\lambda\mathbf{k}}^{\dagger}$ and annihilation $c_{\lambda\mathbf{k}}$ operator satisfied the anti-commutator relation⁶:

$$\{c_{\lambda\mathbf{k}}^{\dagger}, c_{\lambda'\mathbf{k}'}^{\dagger}\} = \{c_{\lambda\mathbf{k}}, c_{\lambda'\mathbf{k}'}\} = 0; \quad \{c_{\lambda\mathbf{k}}, c_{\lambda'\mathbf{k}'}^{\dagger}\} = \delta_{\lambda\lambda'} \delta_{\mathbf{k}\mathbf{k}'}$$

⁶ $\{A, B\} = AB + BA$

The coulomb interaction matrix elements:



$$V_{\mathbf{k}, \mathbf{k}', \mathbf{q}}^{\alpha\beta\gamma\delta} = \langle \psi_{\alpha\mathbf{k}+\mathbf{q}} \psi_{\beta\mathbf{k}'-\mathbf{q}} | V_{ee} | \psi_{\gamma\mathbf{k}} \psi_{\delta\mathbf{k}'} \rangle = \delta^{\gamma\alpha} \delta^{\beta\delta} \quad (11)$$

$$= \int \frac{d^3r}{V} \int \frac{d^3r'}{V} e^{-i\mathbf{q}(\mathbf{r}-\mathbf{r}')} u_{\alpha\mathbf{k}+\mathbf{q}}^*(\mathbf{r}) u_{\beta\mathbf{k}-\mathbf{q}}^*(\mathbf{r}') V_{ee} u_{\gamma\mathbf{k}'}(\mathbf{r}') u_{\delta\mathbf{k}}(\mathbf{r}),$$

With the 3-D Coulomb interaction have the form:

$$V_{ee}(\mathbf{r}) = \frac{e^2}{\varepsilon|\mathbf{r}|} \quad (12)$$

Using Fourier transform for the potential, apply long-wave approximation and take the limit $z \rightarrow 0$ to have the 2-D Coulomb matrix elements:

$$V_{\mathbf{k}, \mathbf{k}', \mathbf{q}}^{\alpha\beta\gamma\delta} = \frac{e^2}{2\epsilon L^2} \frac{1}{|\mathbf{q}_{\parallel}|} \langle u_{\alpha\mathbf{k}+\mathbf{q}} | u_{\delta\mathbf{k}} \rangle \langle u_{\beta\mathbf{k}'-\mathbf{q}} | u_{\gamma\mathbf{k}'} \rangle \quad (13)$$

From the equations of motion (in Heisenberg's picture) for $c_{\mathbf{k}}^{\dagger}c_{\mathbf{k}}$, we have the equations of motion for the expected value $\langle c_{\mathbf{k}}^{\dagger}c_{\mathbf{k}} \rangle$:

$$\begin{aligned}
 \frac{d\langle c_{\mathbf{k}}^{\dagger}c_{\mathbf{k}} \rangle}{dt} &= -\frac{i}{\hbar} \left\langle \left[H^0 + H^{Coul.} + H_{e-L}, c_{\mathbf{k}}^{\dagger}c_{\mathbf{k}} \right] \right\rangle \\
 &= \frac{i}{\hbar} (\varepsilon_{\lambda}(\mathbf{k}) - \varepsilon_{\lambda'}(\mathbf{k})) \langle c_{\mathbf{k}}^{\dagger}c_{\mathbf{k}} \rangle + \left\langle \left[H_{e-L}, c_{\mathbf{k}}^{\dagger}c_{\mathbf{k}} \right] \right\rangle \\
 &\quad + \frac{i}{\hbar} \sum_{\mathbf{k}'\mathbf{q}} \sum_{\alpha\beta\gamma} V_{\mathbf{k},\mathbf{k}',\mathbf{q}}^{\alpha\beta\gamma\lambda} \langle c_{\alpha\mathbf{k}+\mathbf{q}}^{\dagger} c_{\beta\mathbf{k}'-\mathbf{q}}^{\dagger} c_{\gamma\mathbf{k}'} c_{\lambda'\mathbf{k}} \rangle \\
 &\quad + \frac{i}{\hbar} \sum_{\mathbf{k}'\mathbf{q}} \sum_{\alpha\gamma\delta} V_{\mathbf{k}',\mathbf{k}+\mathbf{q},\mathbf{q}}^{\alpha\lambda'\gamma\delta} \langle c_{\lambda\mathbf{k}}^{\dagger} c_{\alpha\mathbf{k}'+\mathbf{q}}^{\dagger} c_{\gamma\mathbf{k}+\mathbf{q}} c_{\delta\mathbf{k}'} \rangle
 \end{aligned} \tag{14}$$

Approximation the expected value of four-operator by multiplication of two expected value (Hartree-Fock Approximation):

$$\begin{aligned}
 \langle c_{\alpha\mathbf{k}+\mathbf{q}}^{\dagger} c_{\beta\mathbf{k}'-\mathbf{q}}^{\dagger} c_{\gamma\mathbf{k}'} c_{\lambda'\mathbf{k}} \rangle &\approx -\langle c_{\alpha\mathbf{k}+\mathbf{q}}^{\dagger} c_{\gamma\mathbf{k}'} \rangle \langle c_{\beta\mathbf{k}'-\mathbf{q}}^{\dagger} c_{\lambda'\mathbf{k}} \rangle \delta_{\mathbf{k}+\mathbf{q},\mathbf{k}'} \\
 \langle c_{\lambda\mathbf{k}}^{\dagger} c_{\alpha\mathbf{k}'+\mathbf{q}}^{\dagger} c_{\gamma\mathbf{k}+\mathbf{q}} c_{\delta\mathbf{k}'} \rangle &\approx \langle c_{\lambda\mathbf{k}+\mathbf{q}}^{\dagger} c_{\delta\mathbf{k}'} \rangle \langle c_{\alpha\mathbf{k}'+\mathbf{q}}^{\dagger} c_{\gamma\mathbf{k}+\mathbf{q}} \rangle \delta_{\mathbf{k}',\mathbf{k}}
 \end{aligned} \tag{15}$$

Substituting (15) into (14) and doing some transformations on the light-matter interaction part to have

$$\begin{aligned} \frac{d \langle c_{\lambda \mathbf{k}}^\dagger c_{\lambda' \mathbf{k}} \rangle}{dt} &= \frac{i}{\hbar} (\varepsilon_\lambda(\mathbf{k}) - \varepsilon_{\lambda'}(\mathbf{k})) \langle c_{\lambda \mathbf{k}}^\dagger c_{\lambda' \mathbf{k}} \rangle \\ &\quad - \frac{i}{\hbar} \sum_\mu \left(\Sigma_{\mu\lambda}(\mathbf{k}) \langle c_{\mu \mathbf{k}}^\dagger c_{\lambda' \mathbf{k}} \rangle - \langle c_{\lambda \mathbf{k}}^\dagger c_{\mu \mathbf{k}} \rangle \Sigma_{\mu\lambda'}(\mathbf{k}) \right) \end{aligned} \quad (16)$$

in which

$$\Sigma_{\mu\nu} = \frac{e\mathbf{A}(t)}{m} \mathbf{p}_{\mu\nu}(\mathbf{k}) - \sum_{\alpha\beta\mathbf{q}} V_{\mathbf{k},\mathbf{k}+\mathbf{q},\mathbf{q}}^{\alpha\mu\beta\nu} \rho_{\alpha\beta}(\mathbf{k}+\mathbf{q}) \quad (17)$$

$$\mathbf{p}_{\mu\nu} = \frac{m}{\hbar} \langle u_{\lambda\mathbf{k}} | \nabla_{\mathbf{k}} H_{1e}^0(\mathbf{k}) | u_{\lambda'\mathbf{k}} \rangle \quad (18)$$

$$H_{1e}^0(\mathbf{k}) = e^{-i\mathbf{k}\mathbf{r}} H_{1e}^0(\mathbf{r}) e^{i\mathbf{k}\mathbf{r}} = e^{-i\mathbf{k}\mathbf{r}} \left(\frac{\mathbf{p}^2}{2m} + V_0(\mathbf{r}) \right) e^{i\mathbf{k}\mathbf{r}} \quad (19)$$

Equation (16) can describe the transition band between valence bands and conduction bands, but lack of relaxation effect.

For a better realistic picture, we taken into account the correction from the scattering effect:

$$\left(\frac{d\rho(\mathbf{k})}{dt} \Big|_{scat.} \right)_{\lambda\lambda'} \rightarrow -\frac{\rho_{\lambda\lambda'}(\mathbf{k})}{T_2} (1 - \delta_{\lambda\lambda'}) \quad (20)$$

The parameter T_2 can be choosing to fit with the experiment, or confirms the exist of the exciton in the absorption spectrum.

Finally, we have the semiconductor Bloch equations⁷:

$$\begin{aligned} \frac{d\rho_{\lambda\lambda'}(\mathbf{k})}{dt} = & \frac{i}{\hbar}(\varepsilon_{\lambda}(\mathbf{k}) - \varepsilon_{\lambda'}(\mathbf{k}))\rho_{\lambda\lambda'}(\mathbf{k}) \\ & - \frac{i}{\hbar} \sum_{\mu} \left(\Sigma_{\mu\lambda}(\mathbf{k}) \langle c_{\mu\mathbf{k}}^{\dagger} c_{\lambda'\mathbf{k}} \rangle - \langle c_{\lambda\mathbf{k}}^{\dagger} c_{\mu\mathbf{k}} \rangle \Sigma_{\mu\lambda'}(\mathbf{k}) \right) \\ & - \frac{\rho_{\lambda\lambda'}(\mathbf{k})}{T_2} (1 - \delta_{\lambda\lambda'}), \end{aligned} \quad (21)$$

where,

$$\Sigma_{\mu\nu} = \frac{e\mathbf{A}(t)}{m} \mathbf{p}_{\mu\nu}(\mathbf{k}) - \sum_{\alpha\beta\mathbf{q}} V_{\mathbf{k},\mathbf{k}+\mathbf{q},\mathbf{q}}^{\alpha\mu\beta\nu} \rho_{\alpha\beta}(\mathbf{k}+\mathbf{q}) \quad (22)$$

⁷Haug and Koch, *Quantum Theory Of The Optical And Electronic Properties Of Semiconductors (fifth Edition)*.

Dipole matrix elements can be obtained through:

$$\vec{\xi}_{\mu\nu}(\mathbf{k}) = \frac{-i\hbar}{m} \frac{\mathbf{p}_{\mu\nu}(\mathbf{k})}{\varepsilon_{\mu}(\mathbf{k}) - \varepsilon_{\nu}(\mathbf{k})}. \quad (23)$$

for $\mu \neq \nu$

Time-dependent interband polarization density:

$$\mathbf{P}(t) = \frac{e}{L^2} \sum_{\mathbf{k}} \text{Tr} \left[\vec{\xi}(\mathbf{k}) \rho(\mathbf{k}, t) \right] \quad (24)$$

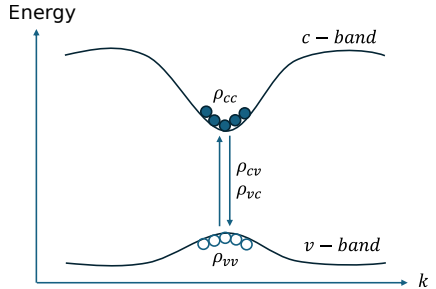


Figure: Density matrix element illustration

Three-band Tightbinding model

Use basic functions of d-type orbitals:

$$|\phi_1\rangle = d_{z^2}, |\phi_2\rangle = d_{xy}, |\phi_3\rangle = d_{x^2-y^2}.$$

Three-band TB Hamiltonian with SOC has the form:

$$H_{6\times 6}^{TB}(\mathbf{k}) = \begin{bmatrix} H_{3\times 3}^{TB}(\mathbf{k}) + \gamma L_z & 0 \\ 0 & H_{3\times 3}^{TB}(\mathbf{k}) - \gamma L_z \end{bmatrix}, \quad L_z = \begin{bmatrix} 0 & 0 & 0 \\ 0 & 0 & i \\ 0 & -i & 0 \end{bmatrix}.$$

Numerical Evaluation of The Sum Over k-space

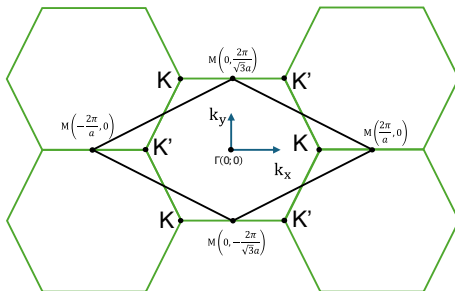
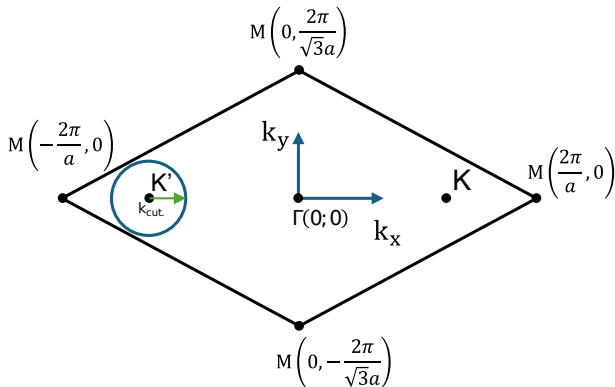


Figure: Rhombus primitive cell

$$\sum_{\mathbf{k}} \dots \rightarrow \frac{L^2}{4\pi^2} \int \int_{BZ} dk_x dk_y \dots \quad (25)$$

k-Cutoff



For k-points around K' point

$$W_{\mathbf{k}, \mathbf{k}', \mathbf{q}}^{\alpha\mu\beta\nu} \approx W_{\mathbf{k}, \mathbf{k}', \mathbf{q}}^{\alpha\mu\beta\nu} \theta(k_{cut.} - |\mathbf{k} - \mathbf{k}_{K'}|) \theta(k_{cut.} - |\mathbf{k}' - \mathbf{k}_{K'}|). \quad (26)$$

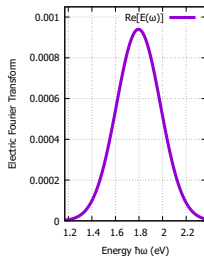
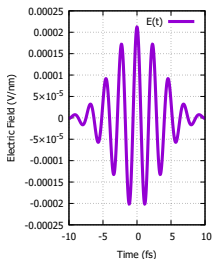
The same for k-points around K point

Electromagnetic Field

The electric field has a Gaussian envelope form:

$$\mathbf{E}(t) = \mathbf{E}_0 \cos(\omega_0 t) e^{-\frac{t^2}{\tau_L^2}} \quad (27)$$

- small $E_0 : \rho_{cc}(\mathbf{k}) \rightarrow 0$
- $\hbar\omega_0 = E_{gap}$.
- small $\tau_L \rightarrow$ rounder Fourier transform's peak around ω_0



Absorption coefficient⁸:

$$\alpha(\omega) \propto \frac{P(\omega)}{E(\omega)}. \quad (28)$$

⁸Haug and Koch, *Quantum Theory Of The Optical And Electronic Properties Of Semiconductors (fifth Edition)*.

Experiment measure:

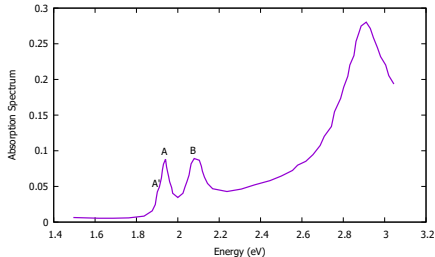


Figure: Measured Absorption Spectrum of MoS_2 at $T = 5\text{K}$ extracted from Ref.⁹

$$E_{\text{gap}} = 2.15 \pm 0.06 \text{ eV}$$

Binding energy:

$$E_{\text{bind.}} = E_{\text{gap}} - E_A = 0.22 \text{ eV}$$

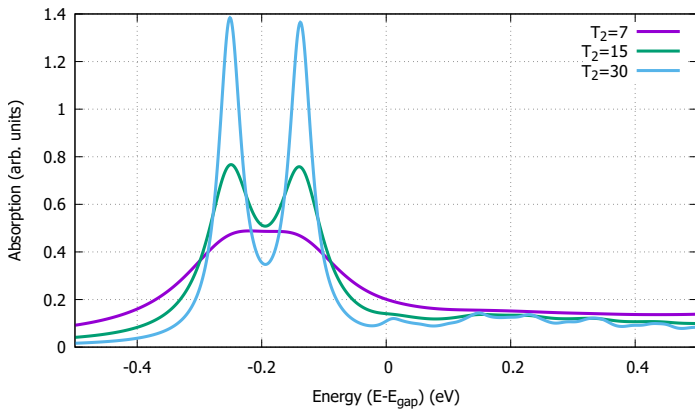
From this figure, we see

- Two resonance labeled by A (1.93 eV) and B (2.1 eV) are exciton peaks (band split due to SOC)
- Weak trion peak near A labeled by A' (18 meV)

To fit with experiment, we can change:

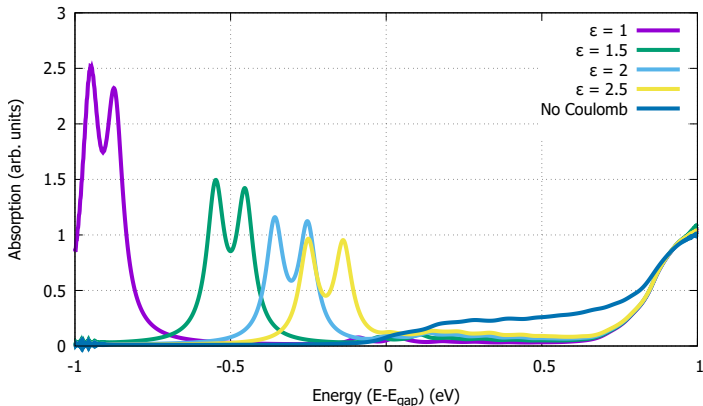
- Relative permittivity ϵ
- Dephasing time T_2

⁹Zhang et al., “Absorption of light by excitons and trions in monolayers of metal dichalcogenide MoS_2 ”.



Choosing the T_2 for clearer Exciton peak:

- The bigger T_2 , the clearer main Exciton peaks \rightarrow confirm two peak.
- At $T_2 = 30$ fs show other smaller peaks \rightarrow predict other peaks.



- Choosing the ϵ for fitting with the experiment.
- For 3-band TB model: $\epsilon \in (1.5, 2.5)$ is in good agreement with measurement binding energy of $E_{bind.} = 0.2 - 0.5 eV$ ¹⁰

¹⁰Zhang et al., “Absorption of light by excitons and trions in monolayers of metal dichalcogenide MoS_2 ”.

Summary:

- From three-band TB + SBE \rightarrow Linear Absorption Spectrum.
- We confirm the Exciton binding energy in this model is in agreement with experimental data, and predict smaller exciton peaks.

Further research:

- High Harmonic Generation
- High-order Side-band Generation
- Photovoltaic effect

Thank you for your listening.



Ataca, C., H. Şahin, and S. Ciraci. “Stable, Single-Layer MX₂ Transition-Metal Oxides and Dichalcogenides in a Honeycomb-Like Structure”. In: (2012).



Diakite, Yacouba Issa et al. *Accurate Electronic, Transport, and Bulk Properties of Gallium Arsenide (GaAs)*. 2016.



Haug, Hartmut and Stephan W. Koch. *Quantum Theory Of The Optical And Electronic Properties Of Semiconductors (fifth Edition)*. en. Google-Books-ID: 1J1IDQAAQBAJ. Jan. 2009.



Liu, Gui-Bin et al. “Electronic structures and theoretical modelling of two-dimensional group-VIB transition metal dichalcogenides”. In: (2015).



Liu, Gui-Bin et al. “Three-band tight-binding model for monolayers of group-VIB transition metal dichalcogenides”. In: (2013).



Radisavljevic, B. et al. “Single-layer MoS₂ transistors”. In: (2011).



Zhang, Changjian et al. “Absorption of light by excitons and trions in monolayers of metal dichalcogenide MoS₂: Experiments and theory”. In: *Phys. Rev. B* 89.20 (May 2014). Publisher: American Physical Society, p. 205436.